# Multi-point Padè for the study of phase transitions: from the Ising model to lattice QCD

**Francesco Di Renzo**[*] **and Simran Singh**

*Dipartimento di Scienze Matematiche, Fisiche e Informatiche, Università di Parma*
*and INFN, Gruppo Collegato di Parma, I-43100, Parma, Italy*

*E-mail:* francesco.direnzo@unipr.it, simran.singh@unipr.it

The Bielefeld Parma collaboration has recently put forward a method to investigate the QCD phase diagram based on the computation of Taylor series coefficients at both zero and imaginary values of the baryonic chemical potential. The method is based on the computation of multi-point Padé approximants. We review the methodological aspects of the computation and, in order to gain confidence in the approach, we report on the application of the method to the two-dimensional Ising model (probably the most popular arena for testing tools in the study of phase transitions). Besides showing the effectiveness of the multi-point Padé approach, we discuss what these results can suggest in view of further progress in the study of the QCD phase diagram. We finally report on very preliminary results in which we look for Padé approximants at different temperatures and fixed values of the (imaginary) baryonic chemical potential.

*The 39th International Symposium on Lattice Field Theory (Lattice2022),*
*8-13 August, 2022*
*Bonn, Germany*

---

[*]Speaker

## 1. How it all began: from Taylor expansions on thimbles to imaginary $\mu_B$ LQCD

The QCD phase diagram is still to a large extent elusive: in particular, due to the so-called sign problem, the lattice (the non-perturbative tool which would be supposed to provide valuable insight) cannot probe the relevant regions in the $T - \mu_B$ (Temperature-baryonic chemical potential) plane. In the last couple of years, the Bielefeld-Parma collaboration put forward a method to compute finite-density QCD thermodynamic observables in the region to which access would be precluded by the sign problem; this approach is also able to probe the singualrity structure of the theory in the complex $\mu_B$ plane [1–4]. The method is based on the computation of Taylor series coefficients at both zero and imaginary values of the baryonic chemical potential, which enables the computation of multi-point Padé approximants. This work aims to assess the effectiveness of the method by making use of it in the context of a very standard playground for the physics of phase transitions (*e.g.* the 2d Ising model). At the same time, we present (very) preliminary results on new applications in the context of finite-density QCD.

Before entering the main subject, it is useful to recall when the idea of applying multi-point Padé rational approximants first came to our mind; that was in the context of thimble regularisation. The latter [5, 6] was introduced to solve (or at least tame) the sign problem by re-expressing the path integral as a sum of integrals computed on manifolds different from the original one. After complexifying the degrees of freedom, one considers the so-called Lefschetz thimbles, *i.e.* the manifolds that are the union of the steepest ascent paths stemming from the various stationary points of the action. On such manifolds the imaginary part of the action stays constant, so that the sign problem reduces to the so-called *residual phase* which is there due to the Jacobian of the change of variables. There is a thimble attached to each stationary point and in principle all can give a contribution to the path integral. This is referred to as the *thimble decomposition*. To make a long story short, we recall that *(a)* not all the thimbles give a non-null contribution, *(b)* this picture changes in different regions of the parameters space of the theory (*i.e.* a given thimble can contribute to the path integral in a region and not in another one) and *(c)* there are cases in which a single thimble (usually the so called *dominant* one, attached to the stationary point with the lowest action) is enough to compute the answer one is interested in. The latter observation gave raise to the *single thimble dominance* hypothesis, which was shown to hold in a few cases, but failed in others. The first example of a failure was provided by the 1-D Thirring model [7, 8], where it was clearly shown that a single thimble is not enough to account for the known analytic result. It is nevertheless important to remark that there are regions in which one single thimble is enough, and this was the logical starting point for the success of a computation based on multi-point Padé rational approximants. The success of such approach [9] can be recognised in Fig. 1. On the left, we display the known analytic result for the chiral condensate $\bar{\chi}\chi$ of the 1-D Thirring model ($L = 8$, $m = 1$, $\beta = 1$) at various values of the chemical potential by mass ratio $\frac{\mu}{m}$. This is plotted together with the numerical results which we got: triangles are results computed on one single thimble at points where we are able to show that this is enough; dots are results taken from the multi-point Padé method that we will better describe in the next section. Here it is enough to say that a few Taylor expansion coefficients were computed at the points marked by triangles and from those the multi-point Padé approximant was computed. The right panel of the figure shows

how the singularity pattern of the solution was reconstructed: the rational approximant displayed a singularity which falls on top of the analytic one. Convergence radii of the Taylor expansions we computed can be spotted, showing that there is an intersection of convergence disks, validating the procedure of bridging the two regions where we were able to compute single thimble results: all in all, while the thimble decomposition is discontinuous, the physical observable is not. The figure refers to a given choice of lattice size, mass and $\beta$-value; we were able to show [10] that the method can successfully account for the extraction of the continuum limit.
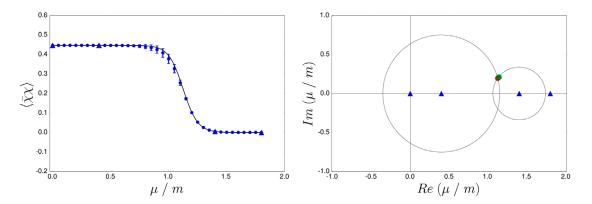


**Figure 1:** Left panel: (continuum line) analytic solution for the condensate $\bar{\chi}\chi$ of the 1-D Thirring model ($L = 8$, $m = 1$, $\beta = 1$) at various values of the chemical potential by mass ratio $\frac{\mu}{m}$; (triangles) numerical results obtained on one single thimble; (dots) numerical results taken from the rational approximant. Right panel: we plot in the complex $\frac{\mu}{m}$ plane the singularity we got from the rational approximant; it is depicted on top of the known analytic one.

## 2. Multi-point Padè method for finite density Lattice QCD

### 2.1 Basics of the multi-point Padè method

Suppose we know a few Taylor expansion coefficients of a given function $f(z)$ at different points $\{z_k \mid k = 1 \ldots N\}$. The basic idea of our multi-point Padé approach is to approximate $f(z)$ by a rational function $R_n^m(z)$, which we call a $[m/n]$ Padé approximant

$$R_n^m(z) = \frac{P_m(z)}{\tilde{Q}_n(z)} = \frac{P_m(z)}{1 + Q_n(z)} = \frac{\sum\limits_{i=0}^{m} a_i z^i}{1 + \sum\limits_{j=1}^{n} b_j z^j}. \tag{1}$$

$R_n^m(z)$ (*i.e.* the $a_i$, $b_j$ coefficients defining it) can be fixed by requiring that it reproduces the values of $f$ and a few of its derivatives at the given points $\{z_k\}$. Provided that $n + m + 1 = Ns$ ($f^{(s-1)}$ being the highest order derivative we computed at each point), this is possible by requiring that

$$\cdots$$
$$P_m(z_k) - f(z_k)Q_n(z_k) = f(z_k)$$
$$P'_m(z_k) - f'(z_k)Q_n(z_k) - f(z_k)Q'_n(z_k) = f'(z_k) \tag{2}$$
$$\cdots$$

3

In Eq. (2) we only wrote 2 out of $s$ equations for 1 out of $N$ points. It should be clear what the overall problem amounts to: we have to solve a linear system, the unknowns being the $\{a_i, b_j \mid i = 1 \ldots m, j = 1 \ldots n\}$. This is not the only possible way to solve for $R_n^m(z)$, but for the purpose of understanding our approach it suffices (the interested reader can refer to [4] for other alternatives[1]). It should be clear that

- Not only $R_n^m(z)$ can reproduce our input pieces of information; by a natural *analytic continuation* it can *predict* values of $f$ in an extended region (to the extent we do not exit the region in which the approximation holds, which thing of course deserves care of its own): left panel of Fig. 1 is an example.

- When a *zero* in the denominator of $R_n^m(z)$ is not canceled by a corresponding zero of the numerator, we face a *singularity* of the rational approximation, which is supposed to teach us something on the *singularity structure* of $f$; quite obviously, singularities live in the *complex z plane*: right panel of Fig. 1 is an example.

## 2.2 First application of the multi-point Padè method to finite density LQCD

In [4] the Bielefeld Parma collaboration applied the multi-point Padè method to finite density LQCD. In the example of section 1 we did not have a way to safely compute the 1D Thirring condensate in regions where more than one thimble give a contribution; on the other hand, we could safely compute (on a single thimble) at given values of $\frac{\mu}{m}$. This is the same as in LQCD: the sign problem does not allow us to compute observables at *real* values of the baryonic chemical potential $\mu_B$, but computations are safe at $\mu_B = 0$ and at *imaginary* values of $\mu_B$ (in particular, we can compute a few orders of the Taylor expansion of an observable). For (2+1)-flavor of highly improved staggered quarks (HISQ) [11] with imaginary chemical potential, we computed cumulants of the net baryon number density, given as

$$\chi_{nB}(T, V, \mu_B) = \left( \frac{\partial}{\partial \hat{\mu}_B} \right)^n \frac{\ln Z(T, V, \mu_l, \mu_s)}{VT^3}, \tag{3}$$

with $\hat{\mu}_B = \mu_B/T$ and $l, s$ referring to light and strange flavors. Dependence on masses is not made explicit: the light to strange ratio is the physical one. By computing at different imaginary values of $\hat{\mu}_B$ (including $\hat{\mu}_B = 0$) we could implement the program of subsection 2.1. Fig. 2 is the counterpart of Fig. 1. We point out that

- In the left panel we can see how well the rational approximants for the number density $\chi_{1B}$ describe data at different temperatures. Actually we show two different rational approximants (enforcing parity or not): they are both fine. The big spike is expected to be there: it is related to the Roberge Weiss transition, and it occurs at the temperature which is supposed to be the relevant one ($T_{RW}$). Minor spikes can be also spotted: they are harmless, and they can be understood in terms of what we will explain in the next section (partial cancellation of zeros between numerator and denominator).

---

[1]Notice that this is the simplest setting also with respect to another point: there is no reason for strictly asking knowledge of the same number of derivatives at each point.
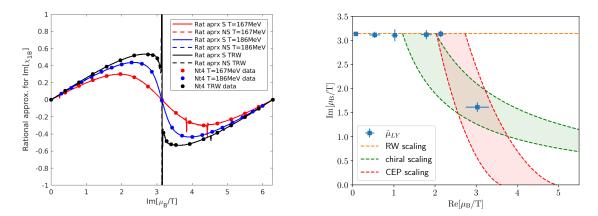
**Figure 2:** (Left panel) The number density $\chi_{1B}$ at various values of $\hat{\mu}_B$ and different temperatures $T$. Data are shown together with two different rational approximants (enforcing parity or not): both describe data very well. The big spike is expected: it is the hint for the Roberge Weiss transition. (Right panel) The singularity pattern in the complex $\hat{\mu}_B$, highlighting their expected overall compliance with Roberge Weiss, chiral and Critical End Point scaling.

- In the right panel we display the singularities we found at different temperatures, relating them to the expected singularity scaling pattern. These are the expected Lee-Yang singularities: one expects a given scaling for the singularities connected to the Roberge Weiss transition, to the chiral transition and to the QCD Critical End Point. While the last two are still under investigation[2], one can clearly see a consistent picture for the Roberge Weiss scaling: indeed in [4] we were able to show that it is the expected one.

All in all, results are intriguing. That's why we now want to show that the machinery is under control for the the most popular arena for testing tools in the study of phase transitions, *i.e.* the two-dimensional Ising model.

## 3. Testing the method on the 2d Ising model

Lee-Yang theory is one of the possible approach to the study of phase transitions. For an example of its application, we refer the interested reader to [12], where the authors study the 2d Ising model. We will basically follow their program, but will not rely on the study of many different cumulants (as they do). We will instead make use of our multi-point Padè method and study only two different cumulants at different values of temperature and magnetic field. The hamiltonian is the well-known one, based on interactions between nearest neighbours and with external magnetic field $h$

$$H = -J \sum_{<i,j>} \sigma_i \sigma_j - h \sum_i \sigma_i \tag{4}$$

---

[2]Indeed we now have an estimate for the CEP Temperature.

with the only possible values $\sigma_i = \pm 1$. In the following $J$ will be set to $J = 1$. The partition function can be written in terms of its *zeros* $\{\beta_k\}$

$$Z(\beta, h) = Z(0, h) \, e^{\beta c} \prod_k (1 - \frac{\beta}{\beta_k}) \tag{5}$$

$c$ being a constant. If we define thermal cumulants by

$$\langle\langle U^n \rangle\rangle = \frac{\partial^n}{\partial(-\beta)^n} \ln Z(\beta, h)$$

it is easy to show that they can be expressed as

$$\langle\langle U^n \rangle\rangle = (-1)^{(n-1)} \sum_k \frac{(n-1)!}{(\beta_k - \beta)^n} \qquad (n > 1) \tag{6}$$

Furthermore, scaling relations describe the approach of leading zeros to critical inverse temperature

$$|\beta_0 - \beta_c| \sim L^{-1/\nu} \qquad \text{Im}(\beta_0) \sim L^{-1/\nu}. \tag{7}$$

In Eq. (7) $\beta_0$ is the Fisher zero, that is the closest zero of the partition function to the real axis, resulting in the closest singularity of cumulants to the real axis[3], $\beta_c$ is the critical inverse temperature and $\nu$ is the relevant critical exponent.

Our program now entails four steps: *(1)* we compute the $n = 2$ thermal cumulant (*i.e.* the specific heat) at various inverse temperatures $\beta$ and lattice sizes $L$; *(2)* for each $L$ we compute the rational approximant $R_n^m(\beta)$ by our multi-point Padè method; *(3)* at each $L$ we find the Fisher zero $\beta_0$, which is obtained as the the closest singularity of the cumulant to the real axis; *(4)* we study the finite size scaling of the values of $\beta_0$. The result of the procedure can be inspected in Fig. 3.
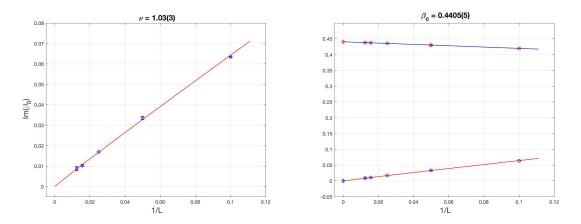


**Figure 3:** (Left panel) The scaling in $1/L$ of $\text{Im}(\beta_0)$, *i.e.* the imaginary part of the Fisher zero, detected as that the closest singularity of the cumulant to the real axis. The correct critical exponent $\nu = 1$ is got with fairly good accuracy. (Right panel) Once $\nu$ has been recognised to be the right one, one can fit the value of the critical inverse temperature $\beta_c$, which is reconstructed to per mille accuracy.

---

[3]$\beta_0$ shows up together with its complex conjugate $\beta_0^*$.

- In the left panel we display the scaling in $1/L$ of $\text{Im}(\beta_0)$. Errors are computed by varying results with respect to statistical errors for the cumulant and functional form for the rational approximant. As one can see, the value of the relevant critical exponent $\nu = 1$ is got with fairly good accuracy (1.03(3)).

- Once $\nu = 1$ has been recognised, we can fit the scaling of the real part $\text{Re}(\beta_0)$ (right panel), thus finding the value of the critical inverse temperature. We get the very accurate result $\beta_c = 0.4405(5)$.

Once the critical inverse temperature is known, one can sit on top of it and study the scaling in $L$ of $\text{Im}(h_0)$, $h_0$ being the Lee Yang zero, that is the closest singularity of a magnetic cumulant to the real axis. Explicitly, our program again entails four steps: *(1)* we compute the $n = 1$ magnetic cumulant (*i.e.* the magnetisation) at $\beta = \beta_c$ and various values of external magnetic field $h$ and lattice size $L$; *(2)* for each $L$ we compute the rational approximant $R_n^m(h)$ for the magnetisation by our multi-point Padè method; *(3)* at each $L$ we find the Lee Yang zero $h_0$, which is the singularity of the rational approximant for the magnetisation which is the closest to the real axis; *(4)* we study the finite size scaling of the values of $\text{Im}(h_0)$ (as we will see, $h_0$ always sits at $\text{Re}(h_0) = 0$).

Before we inspect this scaling behaviour, it is useful to have a closer look at the singularity pattern in the complex $h$ plane at given values of $L$. In Fig 4 we depict the zeros of the numerator (blue crosses) and of the denominator (red circles) of our $R_n^m(h)$ at different values of the lattice size $L$, *i.e.* $L = 15$ (left panel) and $L = 30$ (right panel). We can easily make a couple of key observations.

- A few zeros of the denominator are canceled by corresponding zeros of the numerator. These are not genuine pieces of information: actually their location vary when varying *e.g.* the order of the Padé approximant $[m, n]$. On the other hand, genuine pieces of information (*i.e.* actual zeros and poles) stay constant to a very good precision. Notice that this is the explanation for the small spikes in Fig. 2: they are simply the shadow of cancellations which are indeed very good, but not good enough to be invisible when plotting the rational approximant.
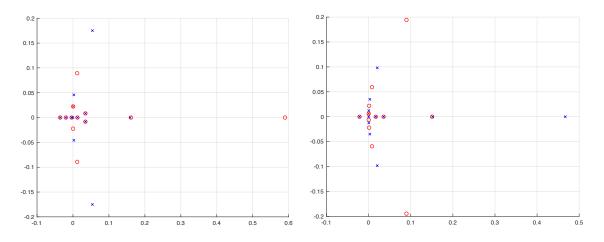


**Figure 4:** (Left panel) Zeros of the numerator (blue crosses) and of the denominator (red circles) of the rational approximant $R_n^m(h)$ for the magnetisation on $L = 15$ (left panel) and $L = 30$ (right panel). We highlight the closest singularity to the real axis, which is getting closer to the real axis itself as $L$ gets larger, with real parts being $\text{Re}(h_0) = 0$. Plots are in the complex $h$ plane.

- We can clearly see that, as the lattice size $L$ gets larger, the closest singularity (Lee Yang zero, highlighted in the plot) gets closer to the real axis, with real parts being $\mathrm{Re}(h_0) = 0$.

Finally, in Fig. 5 we plot the finite size scaling of $\mathrm{Im}(h_0)$. As one can see, the critical exponent in is got with very good accuracy (this time, less than percent: $-1.880(16)$ vs $-1.875$). The steps we could take in the (much simpler) case of the Ising model would be the preferred conceptual path to follow also for LQCD. Needless to say, it will take time before we can be in a position to do that.

## 4. Back to LQCD: a T-Padé application

We finally go back to LQCD for a (very) preliminary account of a new application. Till now we have seen multi-point Padè approximants from data taken at a given temperature $T$ and different values of $\hat{\mu}_B$: with this we mean that we obtained different $R_n^m(\hat{\mu}_B)$ at different $T$ values. With the very same data, we can think of going the other way around, that is we can obtain $R_n^m(T)$ at different $\hat{\mu}_B$ values. Fig. 6 is an example of what we can get following this path. Of course, this time singularities emerge in the complex $T$ plane.

## 5. Conclusions

The multi-point Padè method for the study of phase transitions has already proved to be quite effective in the case of LQCD. Here we showed how the approach can provide very accurate results when collecting a rich statistics is not such a hard numerical task (as it was the case for the 2d Ising
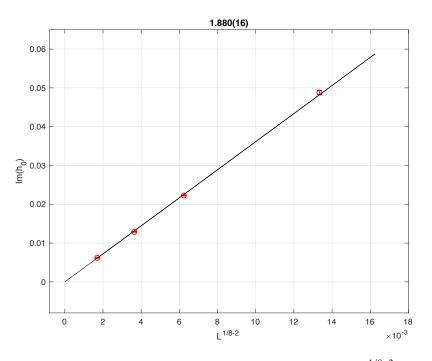


**Figure 5:** Finite size scaling of $\mathrm{Im}(h_0)$. To guide the eye, we plot data versus $L^{1/8-2}$, where the correct critical exponent is taken. As the figure title we report the absolute value of the one we got, which turns out to be a very accurate estimate, to less than percent.
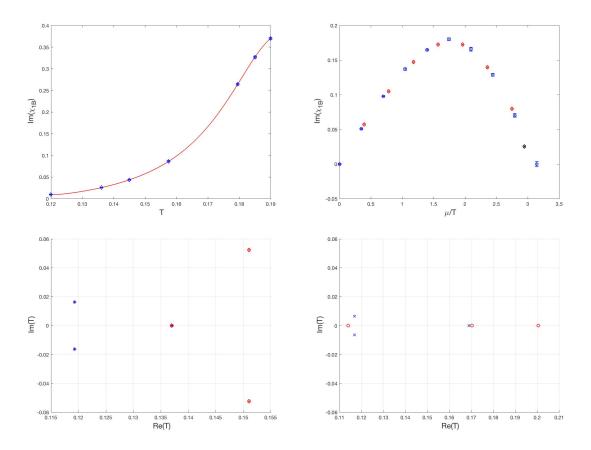
**Figure 6:** (Top-left panel) An example of $R_n^m(T)$ for $\chi_{1B}$ at a given value of $\hat{\mu}_B$ on top of data taken at different temperatures $T$ at the same given value of $\hat{\mu}_B$. (Top-right) Actual measurements of $\chi_{1B}(\hat{\mu}_B)$ at a given temperature $T$ plotted together with interpolating data obtained from $R_n^m(T)$. Everything looks pretty smooth; we plot in a different colour the only data point possibly not falling smoothly on top of actual data. (Bottom-left) Zeros of denominator (red) and zeros of numerator (blue) of $R_n^m(T)$ in the complex $T$ plane at a low value of $\hat{\mu}_B$. (Bottom-right) The same plot at a value of $\hat{\mu}_B$ close to $\hat{\mu}_B = i\pi$ ($T$ is expressed in GeV)

model). This is at same time a proof of concept of the reliability of the method and a stimulus to do better in the case of finite density LQCD.

## Acknowledgements

## References

[1] C. Schmidt, J. Goswami, G. Nicotra, F. Ziesché, P. Dimopoulos, F. Di Renzo et al., *Net-baryon Number Fluctuations*, *Acta Physica Polonica B Proceedings Supplement* **14** (2021) 241.

[2] S. Singh, P. Dimopoulos, L. Dini, F. Di Renzo, J. Goswami, G. Nicotra et al., *Lee-Yang edge singularities in lattice QCD : A systematic study of singularities in the complex $\mu_B$ plane using rational approximations*, *Proceedings of The 38th International Symposium on Lattice Field Theory — PoS(LATTICE2021)* (2022) 544.

[3] G. Nicotra, P. Dimopoulos, L. Dini, F. Di Renzo, J. Goswami, C. Schmidt et al., *Lee-Yang edge singularities in 2 + 1 flavor QCD with imaginary chemical potential*, *Proceedings of The 38th International Symposium on Lattice Field Theory — PoS(LATTICE2021)* (2022) 260.

[4] P. Dimopoulos, L. Dini, F. Di Renzo, J. Goswami, G. Nicotra, C. Schmidt et al., *Contribution to understanding the phase structure of strong interaction matter: Lee-Yang edge singularities from lattice QCD*, *Phys. Rev. D* **105** (2022) 034513 [2110.15933].

[5] AURORASCIENCE collaboration, *New approach to the sign problem in quantum field theories: High density QCD on a Lefschetz thimble*, *Phys. Rev. D* **86** (2012) 074506 [1205.3996].

[6] H. Fujii, D. Honda, M. Kato, Y. Kikukawa, S. Komatsu and T. Sano, *Hybrid Monte Carlo on Lefschetz thimbles - A study of the residual sign problem*, *JHEP* **10** (2013) 147 [1309.4371].

[7] H. Fujii, S. Kamata and Y. Kikukawa, *Monte Carlo study of Lefschetz thimble structure in one-dimensional Thirring model at finite density*, *JHEP* **12** (2015) 125 [1509.09141].

[8] A. Alexandru, G. Basar, P.F. Bedaque, G.W. Ridgway and N.C. Warrington, *Sign problem and Monte Carlo calculations beyond Lefschetz thimbles*, *JHEP* **05** (2016) 053 [1512.08764].

[9] F. Di Renzo, S. Singh and K. Zambello, *Taylor expansions on Lefschetz thimbles*, *Phys. Rev. D* **103** (2021) 034513 [2008.01622].

[10] F. Di Renzo and K. Zambello, *Solution of the Thirring model in thimble regularization*, *Phys. Rev. D* **105** (2022) 054501 [2109.02511].

[11] HPQCD, UKQCD collaboration, *Highly improved staggered quarks on the lattice, with applications to charm physics*, *Phys. Rev. D* **75** (2007) 054502 [hep-lat/0610092].

[12] A. Deger and C. Flindt, *Determination of universal critical exponents using Lee-Yang theory*, *Phys. Rev. Research.* **1** (2019) 023004 [1905.02379].

PoS(LATTICE2022)148